Kinetics of Redox Reactions of Oxidized *p*-Phenylenediamine Derivatives. I

R. C. Baetzold and L. K. J. Tong*

Contribution from the Research Laboratories, Eastman Kodak Company, Rochester, New York 14650. *Received June 2, 1970*

Abstract: Quinonediimine is produced within microseconds when *p*-azidoaniline derivatives are photolyzed in water. Photolysis in the presence of *p*-phenylenediamine derivatives (PPD) permits rate measurements of the reaction PPD + QDI + $H^+ \rightleftarrows$ 2SQ (k_1, forward; k_2, reverse), where QDI represents quinonediimine and SQ represents semiquinone. The reaction becomes PPD + QDI + $H_2O \rightleftarrows$ 2SQ + OH^- (k_3, forward; k_4, reverse) at pH >7. Values of the rate constants for the QDI from *p*-*N*,*N*-diethylazidoaniline in ionic strength 0.188 phosphate buffers are: $k_1 = 2.0 \times 10^{13}$ l.²/(mol² sec), $k_2 = 6.3 \times 10^4$ l./(mol sec), $k_3 = 2.0 \times 10^6$ l./(mol sec), $k_4 = 6.3 \times 10^{11}$ l.²/(mol² sec). The reactions involving k_1 and k_3 are promoted by general-acid species; the back-reactions are subject to general-base catalysis. The mechanism of this reaction is believed to involve donation of a proton from acid in concert with the transfer of an electron from PPD to QDI. Ferrocyanide reacts with QDI according to the mechanism QDI + H^+ + $Fe(CN)_6^{4-} \rightleftarrows$ SQ + $Fe(CN)_6^{3-}$ (k_1, forward; k_2, reverse) and SQ + $Fe(CN)_6^{4-} \rightleftarrows$ PPD + $Fe(CN)_6^{3-}$ (k_3, forward; k_4, reverse). The following constants have been determined for the *N*,*N*-diethyl derivative: $k_1 = 2.8 \times 10^{12}$ l.²/(mol² sec), $k_2 = 2.3 \times 10^6$ l./(mol sec), $k_3 = 9.5 \times 10^4$ l./(mol sec), $k_4 = 9.2 \times 10^6$ l./(mol sec). This scheme describes apparent catalysis of the Michaelis equilibrium by the ferricyanide–ferrocyanide couple at low pH.

The oxidation products of *p*-phenylenediamine and its substituted derivatives (designated as PPD in this article), semiquinone and quinonediimine (designated as SQ and QDI, respectively), have been identified.[1,2] An equilibrium, frequently referred to as the Michaelis equilibrium, eq 1, exists between the oxidized and reduced species. In eq 1, R_1 and R_2 are

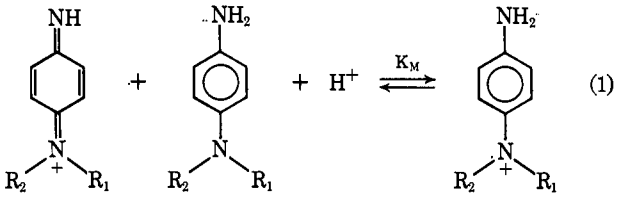

(1)

usually alkyl groups. Equilibrium constants K_M have been reported,[3,4] but no measurements of the rate and mechanism of this reaction are available. Such data would be useful because they would increase understanding of the reaction.

Measurements of the Michaelis equilibrium in aqueous solutions are normally carried out in a flow apparatus because QDI is unstable. The equilibrium concentration of SQ is measured immediately after oxidation of PPD with, *e.g.*, ferricyanide. The time domain imposed by flow systems, however, does not permit rate measurements. In addition, the flash photolysis technique permits us to learn whether the ferrocyanide–ferricyanide couple catalyzes the Michaelis reaction.

When an appropriate phenyl azide is photolyzed in water it forms nitrene,[5] which is quantitatively converted to QDI in a few microseconds (as shown in a later section) according to eq 2. Moreover, photolysis

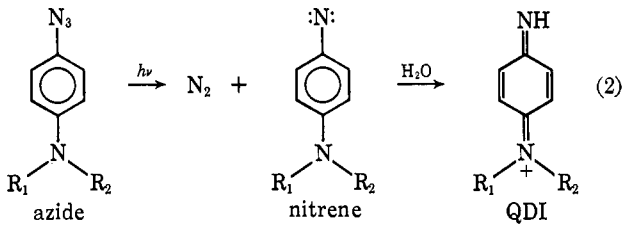

(2)

in the presence of PPD (azide is not an oxidant for PPD) gives us the means to study the rate of the Michaelis reaction (eq 1) by measuring SQ as a function of time. It is this study that concerned us most in this work. An advantage of the photolysis method is that no other redox couple is present (*e.g.*, ferrocyanide, ferricyanide).

Experimental Section

A flash photolysis apparatus has been designed and built for studying kinetics in solution. A variable bank of capacitors (1–8.5 μF) can be charged to 10 kV producing a 400-J flash. The discharge of the capacitors is triggered by a spark gap, which is operated from the amplified delay pulse of an oscilloscope. A xenon-filled flash lamp, mounted parallel to a 10-cm reaction cell, produces the flash, which has a half-life of about 25 μsec. The cell and lamp are housed inside a reflecting metallic box.

The light source in the spectrophotometric part of the apparatus is a 30-W tungsten lamp powered by a 6-V storage battery. Light from this lamp passes through a reaction cell, then a monochromator, and into a photomultiplier tube. An emitter-follower couples the voltage output of the photomultiplier tube to an oscilloscope, where the single sweeps are photographed. The solution in the cell is thermally equilibrated in a bath and the temperature read by a thermistor prior to flashing. Temperature is controlled to $\pm 0.5°$, which is sufficient in view of the low energies of activation involved in these reactions. All rates reported are measured at 25° in aqueous solutions of ionic strength (μ) = 0.188 phosphate buffers. The concentration of azide used in most experiments was 2×10^{-5} *M*, and PPD concentration varied from 3×10^{-5} *M* to 4×10^{-3} *M*. Approximately 25% of the azide is photolyzed by a 200-J flash. At higher concentrations of azide or PPD, problems associated with nonhomogeneous photolysis were observed.

The azides and corresponding PPD's used in this work appear in Chart I. The PPD's were prepared and purified as described in

(1) L. Michaelis, *Chem. Rev.*, 16, 243 (1935).
(2) L. Michaelis, M. P. Schubert, and S. Granick, *J. Amer. Chem. Soc.*, 61, 1981 (1939).
(3) L. K. J. Tong and M. C. Glesmann, *Photogr. Sci. Eng.*, 8, 319 (1964).
(4) J. F. Corbett, *J. Chem. Soc. B*, 207 (1969).
(5) A. Reiser, G. C. Terry, and F. W. Willets, *Nature (London)*, 211, 410 (1966).

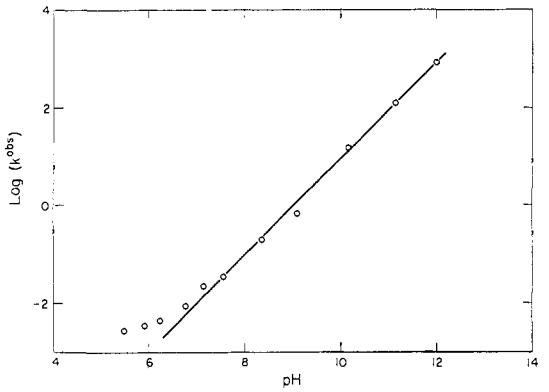

Figure 1. The logarithm of observed rate constant plotted *vs.* pH for deamination of QDI formed by photolyzing azide IV.

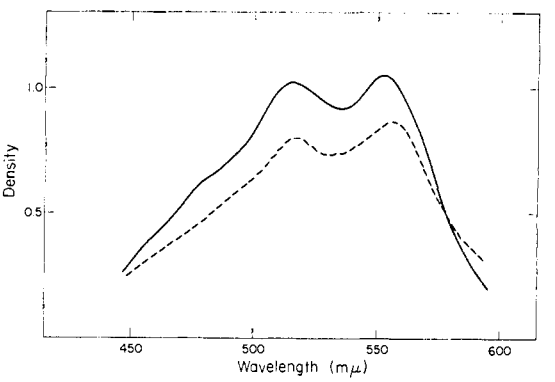

Figure 2. Spectra of SQ IV in water at pH 5.5: ——, formed by ferricyanide oxidation of PPD IV; ---, formed by photolysis of azide IV in the presence of PPD IV.

previous publications from these laboratories.[6] Azides were prepared using a literature procedure.[7] They were recrystallized from 2-propanol when solid or filtered through silica gel when liquid. The elemental analyses are given in Table I.

Chart I. Structures of Azides and PPD's

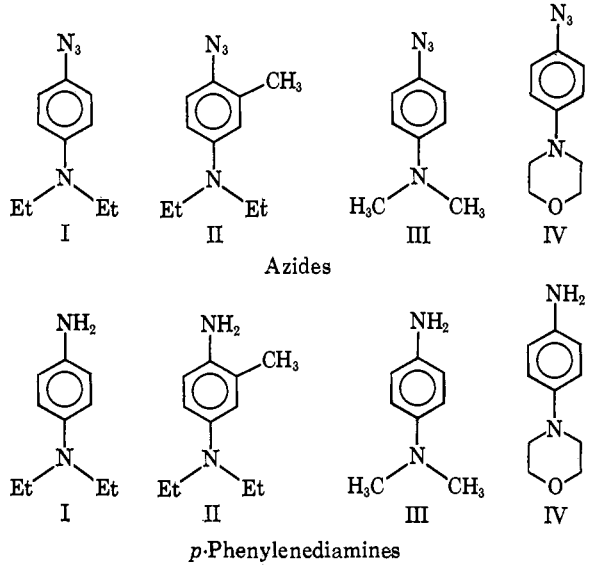

The heat of ionization of PPD was measured by the pH of equimolar mixtures of the acid salt and the free base of PPD at various temperatures.

$$K_R = \frac{[RH^+]}{[R][H^+]} = \frac{\gamma_+}{[H^+]}$$

Assuming that the dependence of the activity coefficient on temperature is not large, ΔH_R is obtained by plotting ln K_R *vs.* reciprocal temperature.

Results

A. QDI Formation. Quinonediimine must be produced faster than it can react by eq 1 in order to demonstrate that the technique of azide photolysis can be used to measure rates of the Michaelis reactions. The ultraviolet absorption spectrum of QDI produced by azide photolysis is partially masked by unreacted azide. At the wavelength 320 mμ an increase in absorption density within the lifetime of the photolysis flash (25 μsec) is observed. This absorption density decreases with time according to first-order kinetics. The rate of decrease is proportional to hydroxide ion concentration (Figure 1) in accordance with the observed[8] deamination kinetics of QDI, and so we attribute the absorption to QDI. Using azide IV, the bimolecular rate constant is 8.91×10^4 l./(mol sec), compared with the reported deamination rate constant for QDI corresponding to PPD IV of 1.00×10^5 l./(mol sec).

Table I

	Azide I		Azide II		Azide III	
	Calcd, %	Found, %	Calcd, %	Found, %	Calcd, %	Found, %
C	63.2	63.3	64.8	65.1	59.2	59.3
H	7.4	7.2	7.9	8.1	6.2	6.4
N	29.4	29.0	27.4	26.8	34.6	34.4

QDI is identified as the aqueous photolysis product of azide by its reaction with phenolic compounds. QDI, formed by chemical oxidation of PPD, reacts with the ionized form of

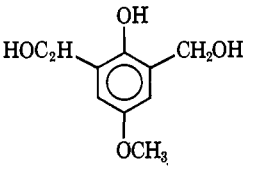

to form azomethine dye with elimination of the methoxy group.[9] The visible absorption spectrum of the dye formed by photolysis of azide II and this coupler is identical with a spectrum of the dye formed from the same phenol and oxidation product of PPD II. The yield of dye formed by repeated photolysis of azide is 95%, indicating that azide can be nearly quantitatively photolyzed to QDI.

As a further check on the photolysis of azide to QDI, the rates in water of dye formation with the above phenolic derivative were compared first using the oxidation product of PPD II, then using the photolytic product of azide II. The rate constants were 2.9×10^4 [10] and 2.4×10^4 l./(mol sec), respectively.

(6) L. K. J. Tong, M. C. Glesmann, and R. L. Bent, *J. Amer. Chem. Soc.*, **82**, 1988 (1960).
(7) W. L. Evans, R. G. D. Moore, and J. E. Redding, *Anal. Chem.*, 34, 159 (1962).
(8) L. K. J. Tong, *J. Phys. Chem.*, **58**, 1090 (1954).
(9) L. K. J. Tong and M. C. Glesmann, *J. Amer. Chem. Soc.*, **79**, 583 (1957).
(10) L. K. J. Tong and M. C. Glesmann, *ibid.*, **90**, 5164 (1968).

The spectrum of the presumed SQ prepared by photolysis of azide IV in the presence of PPD IV is shown in Figure 2. Comparison with the spectrum of the SQ formed by partial oxidation of PPD IV with ferricyanide at low pH shows that the two are identical.

Evidently QDI is formed within a few microseconds during the photolysis of azide in water. Thus, the technique of azide photolysis is useful for studying reaction rates of QDI involving times longer than 25 μsec.

B. Michaelis Reaction. Kinetic Data. A solution for the kinetics of SQ formation is presented here to form a basis for analysis of experimental data. In order not to make any premature commitment on the (H^+) dependence, the latter is incorporated in the rate constants of eq 3.

$$\text{QDI} + \text{PPD} \underset{k_b}{\overset{k_f}{\rightleftharpoons}} 2\text{SQ} \qquad (3)$$

In the mathematical analysis we designate (T) = concentration of QDI, (R) = concentration of PPD, (SQ) = concentration of SQ.

The differential equation representing reaction 3 is

$$\frac{d(SQ)}{dt} = 2k_f(R)(T) - 2k_b(SQ)^2 \qquad (4)$$

In these experiments the concentration of PPD is in excess, making (R) nearly constant. We take into account the protonation of PPD, which occurs at low pH

$$\text{PPD} + H^+ \overset{K_R}{\rightleftharpoons} \text{PPDH}^+ \qquad (5)$$

(where $PPDH^+$ is the protonated form of PPD) in deriving eq 6.

$$(R) = \frac{(\bar{R})}{1 + K_R(H^+)} \qquad (6)$$

where $(\bar{R})$ is the total concentration including all forms of PPD.

Equation 4 is solved by considering the equivalency of oxidized PPD

$$(T)_0 = (T) + (SQ)/2 = (T)_\infty + (SQ)_\infty/2 \qquad (7)$$

where $(T)_0$ is the initial concentration of QDI, $(T)_\infty$ is the final concentration of QDI, $(SQ)_\infty$ is the final concentration of SQ, and the equilibrium condition

$$\left(\frac{d(SQ)}{dt}\right)_{t=\infty} = 0 = 2k_f(R)(T)_\infty - 2k_b(SQ)_\infty^2 \qquad (8)$$

When the results in eq 7 and 8 are substituted into eq 4, eq 9 is obtained.

$$\frac{d(SQ)}{dt} = 2k_b\left[(SQ)_\infty + (SQ) + \frac{k_f(R)}{2k_b}\right] \times [(SQ)_\infty - (SQ)] \qquad (9)$$

The latter equation is integrable by the method of partial fractions and gives

$$d \ln \left(\frac{\beta(SQ)_\infty + (SQ)}{(SQ)_\infty - (SQ)}\right) \Big/ dt = k_f\left(\frac{(\bar{R})}{1 + K_R(H^+)} \frac{4(SQ)}{K_M(H^+)}\right) t = k_{obsd} t \qquad (10)$$

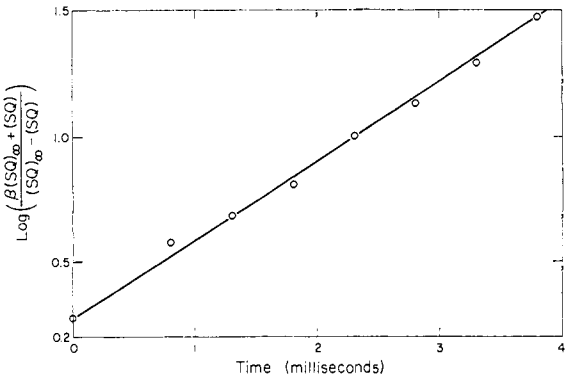

Figure 3. Kinetic data plotted according to eq 10. PPD I = 3.47×10^{-5} M, azide I = 2×10^{-5} M, pH 9.02, β = 1.88.

where we have used the equilibrium constant[3]

$$K_M = k_f/k_b(H^+) \qquad (11)$$

eq 6, and the definition

$$\beta = 1 + \frac{(\bar{R})K_M(H^+)}{2[1 + K_R(H^+)](SQ)_\infty} \qquad (12)$$

The kinetics of SQ formation are first order at low pH in accordance with the behavior of eq 10 for large β. At high pH, published values of K_M are used to evaluate β in making kinetic plots; an example appears in Figure 3.

The rate data obtained from plots similar to that shown in Figure 3 are shown in Table II. The near-

Table II. Observed Rate Data for SQ I Formation

pH	$(\bar{R})$, M	k_{obsd}, sec^{-1}	k_f, l./(mol sec)
6.89	3.47×10^{-5}	17.3	8.00×10^6
6.85	1.39×10^{-4}	77	8.85×10^6
6.89	3.47×10^{-4}	165	7.60×10^6
6.89	1.04×10^{-3}	394	6.05×10^6
4.32	8.15×10^{-5}	16.5	9×10^8
5.05	8.15×10^{-5}	16.5	1.68×10^8
5.62	8.15×10^{-5}	31.5	7.9×10^7
6.15	8.15×10^{-5}	43.3	3.0×10^7
7.09	1.52×10^{-4}	86.6	5.7×10^6
7.57	1.39×10^{-4}	177.5	4.0×10^6
8.29	1.52×10^{-4}	182	3.44×10^6
9.02	3.47×10^{-5}	144	3.13×10^6
9.60	1.39×10^{-4}	770	4.71×10^6

constant value of k_f (defined by eq 10) as concentration of PPD is changed at constant pH (top of Table II) verifies the assumed dependence of k_f on PPD concentration.

The rate constant k_f is dependent on the concentration and type of general-acid species in the system. This effect was determined using inert electrolyte (NaCl) to maintain constant ionic strength while the concentration of buffer was varied (Figure 4). Since early experiments indicated a pH dependence of k_f, pH was kept constant in the experiment of Figure 4. This figure shows the effect of phosphate buffer; other buffers behaved similarly.

The dependence of k_f on buffer ion concentration is analyzed by

$$k_f = k^a_{H_2O} + k^a_{H_3O^+}(H_3O^+) + \sum k^a_{HX}(HX) \qquad (13)$$

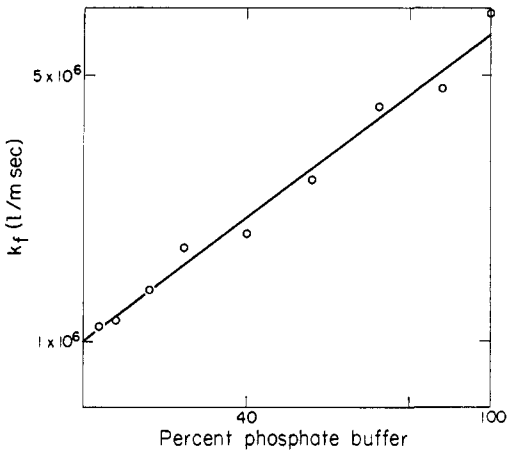

Figure 4. Dependence of SQ I formation rate constant on per cent of ionic strength due to phosphate buffer. Total μ = 0.188, pH 7.00, PPD I = 2.04×10^{-4} *M*.

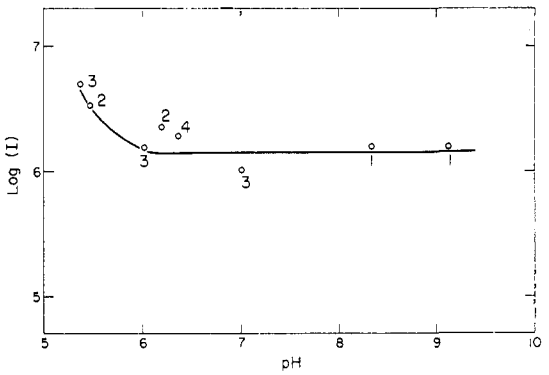

Figure 5. Dependence of intercept of Figure 4 on pH for various anions: 1, carbonate; 2, phosphate; 3, acetate; 4, oxalate.

where the summation extends over each acid species (HX) from the buffer. The result (Figure 4) suggests that a proton from each acid species is involved in each transition state and remains in the products (eq 1). This effect is referred to as promotion by the acid species.

The intercept of Figure 4 equals $k^a_{H_2O} + k^a_{H_3O^+}(H_3O^+)$, according to eq 13. This was demonstrated by the plot of log intercept *vs.* pH for several buffers in Figure 5. The high-pH region corresponds to contributions to the rate due only to $k^a_{H_2O}$. The curvature at low pH is due to the $k^a_{H_3O^+}(H_3O^+)$ term. We evaluated $k^a_{H_2O}$ and $k^a_{H_3O^+}$ from Figure 5.

The rate constants due to each buffer species are determined from slopes of Figure 4 and analogous plots for other ions. When a buffer has several reactive species, slopes at different ratios of buffer ions determine the rate constant for each species. Constants so determined are listed in Table III. These rate constants fit a Brønsted-type relation

$$k_{HX} \propto (K_{HX})^n$$

with $n \cong +0.5$.

The dependence of k_f (eq 13) on concentration of acid species may be used with the equilibrium constant (eq 11) to determine the dependence of k_b on buffer anions. We assume that K_M depends only on total ionic strength, but not the type of ions in the system.

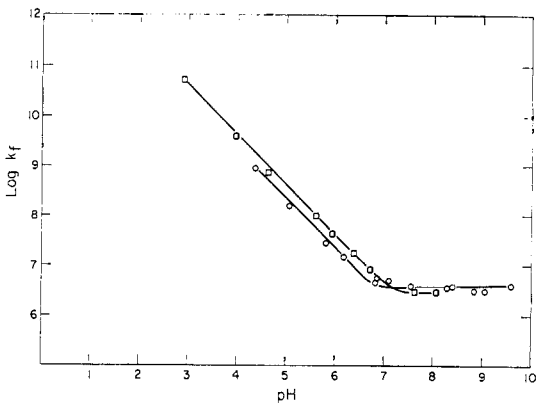

Figure 6. Dependence of SQ formation rate constant on pH: O, azide I; □, azide III.

$$k_b = \frac{k_f}{K_M(H^+)} = k^b_{OH}(OH^-) + k^b_{H_2O} + \sum k_X{}^b(X) \quad (14)$$

where $k^b_{OH} = k^a_{H_2O}/K_M K_W$, $k^b_{H_2O} = k^a_{H_3O^+}/K_M$, $k^b_X = k^a_{HX}/K_M K_{HX}$, and the summation includes all basic species (X) from the buffer. In these definitions K_W is the ion product of water and K_{HX} is the ionization constant for species HX.

Table III. Contributions to k_f Due to Acid Species

Acid species	k^a_{HX}, l.²/(mol² sec)	pK_a
H_3PO_4	6.1×10^{11}	2.12
$HC_2O_4^-$	3.1×10^8	4.28
CH_3COOH	2.0×10^8	4.75
H_2CO_3	3.1×10^9	6.37
$H_2PO_4^-$	8×10^7	7.21
HCO_3^-	1.5×10^7	10.25
HPO_4^{2-}	3.2×10^7	12.67
H_2O	1.0×10^6	14
H_3O^+	1.4×10^{12}	

Figure 6 shows that the Michaelis reaction has two regions of different pH dependence in the phosphate buffer system. In the low-pH region the dominant terms are $k_f = k^a_{H_3O^+}(H_3O^+) + k^a_{H_3PO_4}(H_3PO_4)$ with the corresponding terms in the reverse reaction $k_b = k^b_{H_2O} + k^b_{H_2PO_4^-}(H_2PO_4^-)$. The high-pH region, where Figure 6 is pH independent, is consistent with the dominant terms $k_f = k^a_{H_2O}$ and $k_b = k^b_{OH}(OH^-)$. The rate constants were evaluated from Figure 6 and are listed along with K_M and K_R of each PPD in Table IV for both pH regions.

Activation Energy. The activation energy for the rate of SQ formation at low pH has been measured by Arrhenius-type plots. The observed rate constant is pH independent, as may be seen from eq 10 when PPD is fully protonated, since $k_f = k^a_{H_3O^+}(H_3O^+) + k_{H_3PO_4}(H_3PO_4)$ is proportional to (H^+) in this region. The activation energy measured is given by

$$\frac{d \ln k_{obsd}}{d\, 1/T} = \Delta E = \Delta E_1 - \Delta H_R \quad (15)$$

where ΔE_1 is the activation energy for reaction of QDI with protonated PPD and ΔH_R is the heat of proton-

Table IV. Rate Constants for Michaelis Reaction: Ionic Strength 0.188, Phosphate Buffer

	PPD I	II	III	IV
		Low-pH Region		
$k_f/(H^+)$, l.²/(mol² sec)	2.0×10^{13}	1.0×10^{13}	4.0×10^{13}	1.6×10^{12}
k_b, l./(mol sec)	6.3×10^{4}	1.0×10^{5}	4.0×10^{5}	1.7×10^{5}
		High-pH Region		
k_f, l./(mol sec)	2.0×10^{6}	5.0×10^{5}	2.4×10^{6}	1.6×10^{6}
$k_b/(OH^-)$, l.²/(mol² sec)	6.3×10^{11}	5.1×10^{11}	2.4×10^{12}	1.7×10^{13}
		Equilibrium and Ionization Constants		
K_R, l./mol	1.0×10^{8}	1.4×10^{8}	3.2×10^{6}	1.6×10^{5}
K_M, l./mol	2.9×10^{8}	9.8×10^{7}	1.0×10^{8}	9.6×10^{6} [a]

[a] This value was measured by the technique of ref 3.

Table V. Activation Energies and Heats of Protonation

PPD	ΔE, kcal/mol	ΔH_R, kcal/mol	ΔE_1, kcal/mol
I	6.5	−9.4	−2.9
II	9.7	−9.1	+0.6
III	3.9	−7.0	−3.1
IV	1.76	−5.9	−4.8

ation of PPD. The observed activation energy and the heats of protonation are listed in Table V.

Mechanism. The reaction between QDI and PPD to form SQ is subject to promotion by general acids. This suggests a transition state where the acid is donating a proton as the electron is being transferred from PPD to QDI (X = anion of acid).

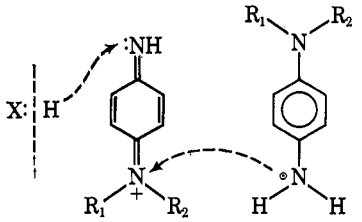

A type of transition state with aromatic rings of PPD and QDI in parallel planes is suggested by the activation energy data, since increasing substitution on tertiary nitrogen or near-primary nitrogen increases the activation energy. This transition state is consistent with a kinetic isotope effect, which is found at pH 6.99 ($k_{H_2O}/k_{D_2O} = 2.03 \pm 0.22$). The transfer of a proton from the acid in the rate-limiting step is a possible explanation for this effect.

C. Reactions of Ferrocyanide with Oxidized PPD. Reactions of QDI are frequently studied[8-11] with the QDI produced by oxidation of PPD with ferricyanide. The equilibrium constant for the oxidation reaction has been reported,[4] but no rate information is available. It is important to determine whether the ferrocyanide–ferricyanide redox couple can influence reaction kinetics of QDI. This is examined by studying the rates of reaction of PPD and its oxidized forms with the $Fe(CN)_6^{4-}$–$Fe(CN)_6^{3-}$ redox couple.

Photolysis of azide I in the presence of ferrocyanide produces QDI, which reacts by eq 16 to form SQ. The SQ is reduced by ferrocyanide in a slower reaction (stage II) to give PPD, as in eq 17. When $Fe(CN)_6^{4-}$

(11) L. K. J. Tong and M. C. Glesmann, *J. Amer. Chem. Soc.*, 79, 592 (1957).

$$QDI + H^+ + Fe(CN)_6^{4-} \underset{k_2}{\overset{k_1}{\rightleftharpoons}} SQ + Fe(CN)_6^{3-} \quad \text{stage I} \quad (16)$$

$$SQ + Fe(CN)_6^{4-} \underset{k_4}{\overset{k_3}{\rightleftharpoons}} PPD + Fe(CN)_6^{3-} \quad \text{stage II} \quad (17)$$

and $Fe(CN)_6^{3-}$ are present in large excess compared with the initial QDI concentration, the differential equation for SQ formation in the first stage is

$$\frac{d(SQ)}{dt} = k_1(T)(H^+)(Fe(CN)_6^{4-}) - k_2(SQ)(Fe(CN)_6^{3-}) \quad (18)$$

The solution to this equation, under pseudo-first-order conditions, is obtained by stoichiometry

$$(T)_0 = (T) + (SQ) \quad (19)$$

and the equilibrium condition

$$\left(\frac{d(SQ)}{dt}\right)_{t=t_f} = 0 = k_1(H^+)(Fe(CN)_6^{4-})(T)_f - k_2(Fe(CN)_6^{3-})(SQ)_f \quad (20)$$

where $(T)_f$ and $(SQ)_f$ are the respective concentrations of QDI and SQ at the time (t_f) when SQ concentration is a maximum; $(T)_0$ was defined before. At time t_f the system is in a state of pseudoequilibrium determined only by stage I; the slower reactions in stage II will be involved in determining the final equilibrium. Equations 19 and 20 are substituted into 18, which gives, upon integration

$$-\frac{d \ln [(SQ)_f - (SQ)]}{dt} = k_1(H^+)(Fe(CN)_6^{4-}) + k_2(Fe(CN)_6^{3-}) = k_{obsd} \quad (21)$$

Appearance of SQ is by first-order kinetics (in accord with eq 21), and three types of experiments have been used to determine rate constants.

1. The reaction involving k_2 is negligible at low pH; we determine $k_1 = 2.69 \times 10^{12}$ l.²/(mol² sec) by the slope of k_{obsd} *vs.* ferrocyanide concentration at low pH.

2. At increased pH, the slope and intercept of the plot k_{obsd} *vs.* ferrocyanide concentration (Figure 7) determines $k_1 = 2.97 \times 10^{12}$ l.²/(mol² sec) and $k_2 = 2.09 \times 10^{6}$ l./(mol sec), respectively.

3. The plot k_{obsd} *vs.* (H^+) (Figure 8) determines $k_1 = 2.72 \times 10^{12}$ l.²/(mol² sec) and $k_2 = 2.48 \times 10^{6}$ l./(mol sec) from slope and intercept, respectively, as predicted by eq 21.

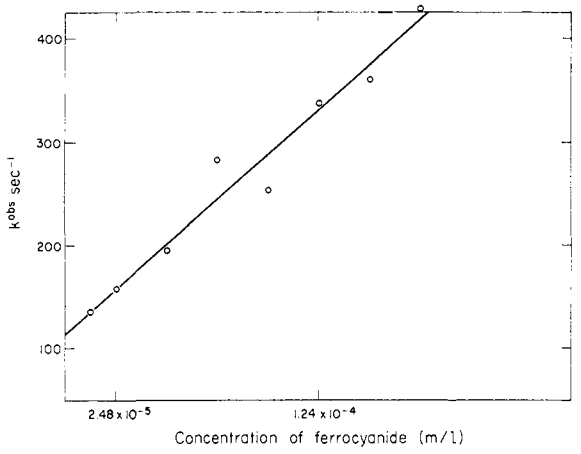

Figure 7. Rate constant for SQ formation from QDI I *vs.* ferrocyanide concentration at pH 6.23 and ferricyanide concentration = 5.52×10^{-5} *M*.

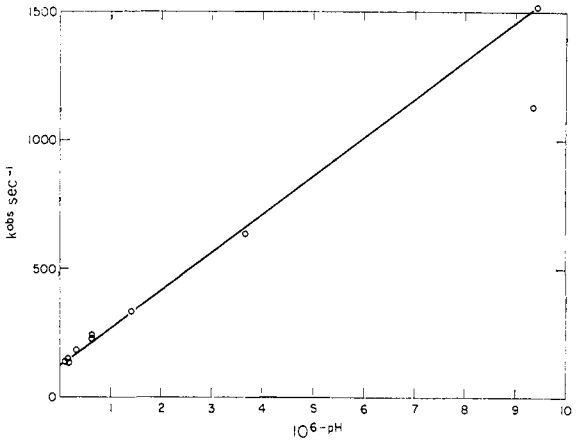

Figure 8. Rate constant for SQ formation from QDI I and 5.45×10^{-5} *M* ferrocyanide *vs.* 10^{6-pH} at 5.25×10^{-5} *M* ferricyanide concentration.

Consider the situation for decay of SQ by stage II when the equilibrium in eq 16 is not completely to the right. The differential equation for SQ decay is

$$-\frac{d(SQ)}{dt} = k_1(H^+)(T)(Fe(CN)_6^{4-}) + k_4(R)(Fe(CN)_6^{3-}) - k_2(Fe(CN)_6^{3-})(SQ) - k_3(Fe(CN)_6^{4-})(SQ) \quad (22)$$

Since reactions in stage I are much faster than reaction 17, the equilibrium is assumed to be maintained by reactions in stage I.

$$\frac{(T)}{(SQ)} = \frac{k_2(Fe(CN)_6^{3-})}{k_1(H^+)(Fe(CN)_6^{4-})} \quad (23)$$

This relation and stoichiometry (eq 24) allow us to simplify and integrate eq 22

$$(T)_0 = (T) + (SQ) + (\bar{R}) \quad (24)$$

to give

$$\frac{-d \ln ((SQ) - (SQ)_\infty)}{dt} = k_{obsd} = k_3(Fe(CN)_6^{4-}) + \frac{k_4(Fe(CN)_6^{3-})}{1 + K_R(H^+)} \frac{k_2k_4}{k_1(H^+)} \frac{(Fe(CN)_6^{3-})^2}{(Fe(CN)_6^{4-})(1 + K_R(H^+))} \quad (25)$$

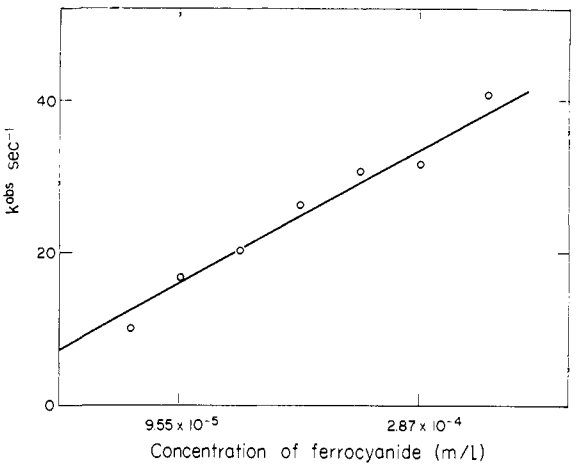

Figure 9. Rate constant for SQ decay by reaction with ferrocyanide *vs.* ferrocyanide concentration at pH 6.23 and ferricyanide concentration = 4.69×10^{-5} *M*.

where $(SQ)_\infty$ is the concentration of SQ at the end of the reaction.

We observe SQ to decay by kinetics in accordance with eq 25. When the observed rate constant is plotted *vs.* ferrocyanide concentration at constant ferricyanide concentration (Figure 9) k_3 and $k_4/(1 + K_R(H^+))$ are obtained from slope and intercept, respectively. We conclude that the term in the rate constant involving both ferrocyanide and ferricyanide concentration is negligible in this experiment. Rate constants calculated by this method are listed in Table VI.

Table VI. Rate Constants for Ferrocyanide–PPD I Reactions

Measured Directly	
k_1	2.8×10^{12} l.^{2}/(mol^2 sec)
k_2	2.3×10^6 l./(mol sec)
k_3	9.5×10^4 l./(mol sec)
k_4	9.2×10^6 l./(mol sec)

Calcd Ratio of Rate Constants	From oxidation potentials	From experimental rates
(k_1/k_2), l./mol	1.55×10^6	1.18×10^6
(k_3/k_4), l./mol	6.75×10^{-3}	1.03×10^{-2}

The equilibrium constants calculated from rate data are compared with those calculated from oxidation potentials[3,4] in Table VI. The oxidation potentials were measured under conditions of ionic strength and buffer type different from those used in these rate measurements. Therefore, only rough agreement is expected. This observed agreement supports the contention that we are measuring rates for reactions 16 and 17. In addition, equilibrium considerations predict that $k_1k_4/k_2k_3 = K_M$. Using the experimentally measured rates, we calculate $k_1k_4/k_2k_3 = 2.3 \times 10^8$ as compared with the published[3] value 2.9×10^8.

The activation energies of the forward reactions in eq 16 and 17 are measured from Arrhenius-type plots. The activation energy for k_3 is found directly to be 11.4 kcal/mol. The activation energy measured for reaction 16 involves a heat of buffer ionization since the rate is pH dependent. The heat of dihydrogen phosphate ionization (ΔH) is taken to be -1.5 kcal/mol from data

in ref 12. The Arrhenius plot has a slope given by

$$\frac{d \ln k_{obsd}}{d 1/T} = \Delta E_1 + \Delta H \quad (26)$$

which gives ΔE_1, the activation energy for reaction involving k_1, the value 6.7 kcal/mol.

Mechanism. The reaction leading to SQ formation in stage I is not subject to promotion by acids as observed for the Michaelis reaction (*i.e.*, plots analogous to that of Figure 4 for this reaction have zero slope). In addition, a kinetic isotope effect ($k_{H_2O}/k_{D_2O} = 1.10 \pm 0.03$) was observed at pH 5.62 by comparison of rates in normal and heavy water. Despite these observations a proton must be involved in the transition state as shown by the dependence of rate on (H^+) in Figure 8.

These observations are consistent with a mechanism involving SQ formation by atomic hydrogen transfer from protonated ferrocyanide[13] through the transition state II. The observed isotope effect is consistent with this mechanism since the experimental pH region is above the pK_a for protonation of ferrocyanide.

The atom transfer would be slower, but the degree of ferrocyanide protonation greater in heavy water than in normal water. Thus, a cancellation could occur giving the observed isotope effect near unity.

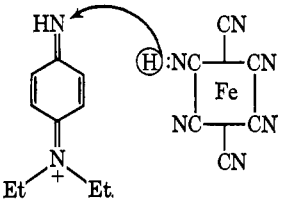

transition state II

The rate data in Tables IV and VI show that $Fe(CN)_6^{4-}$ competes favorably with PPD to reduce QDI at pH below pK_R. Above this pH the order of reactivity is reversed; therefore, ferrocyanide should not exhibit any catalytic effects on the reduction of QDI in the alkaline region. The rate constants for oxidation of PPD by ferricyanide (k_2 and k_4 in Table VI) limit the rate of nucleophilic reactions of QDI which may be studied when QDI is prepared by oxidation of PPD by ferricyanide in the presence of nucleophile.

Acknowledgments. The authors are grateful to Mr. W. Gass of these laboratories for preparation and purification of the azides used in this work, and to Dr. Bryant Rossiter for many helpful discussions.

(12) "Handbook of Chemistry and Physics," 45th ed, Chemical Rubber Publishing Co., Cleveland, Ohio, 1964, p D-79.
(13) I. M. Kolthoff, *J. Phys. Chem.*, **39**, 955 (1935).

Raman Spectra of Dilute Solutions of Some Stereoisomers of Vitamin A Type Molecules

L. Rimai,* D. Gill, and J. L. Parsons

Contribution from the Scientific Research Staff, Ford Motor Company, Dearborn, Michigan 48121. *Received July 23, 1970*

Abstract: Laser-excited Raman spectra of retinals (*trans*, 9-*cis*, 13-*cis*), retinols (*trans*, 13-*cis*), and *trans*-retinoic acid in octanol solution are reported. The terminal group is easily identified by the frequency of the line at 1580–1590 cm^{-1}, while the isomer is uniquely characterized by the lines in the 1100–1400-cm^{-1} range. The observed spectra are mainly contributed by the conjugated segment and not by the saturated part of the molecule. A discussion of possible mode assignments is also presented.

The observation of intense, resonance-enhanced, Raman spectra[1-5] of carotenoids[6] in very dilute solution[7] and in live tissues[8] prompted us to investigate the Raman spectra of a number of vitamin A type molecules.[9-13] The importance of the stereoisomerism of these molecules[14,15] to the mechanism of vision[16-18] and the possibility of identifying stereoisomers by their vibrational spectra[10,19-26] further motivated the present work.

(1) J. Behringer in "Raman Spectroscopy," H. A. Szymanski, Ed., Plenum Press, New York, N. Y., 1967, Chapter 6.
(2) J. Behringer and J. Brandmüller, *Z. Elektrochem.*, **60**, 643 (1956).
(3) A. C. Albrecht, *J. Chem. Phys.*, **33**, 156 (1960).
(4) P. P. Shorygin and T. M. Ivanova, *Dokl. Akad. Nauk SSSR*, **150**, 533 (1963); *Sov. Phys. Dokl.*, **8**, 493 (1963).
(5) T. M. Ivanova, L. A. Yanovskaya, and P. P. Shorygin, *Opt. Spectrosc.*, **18**, 115 (1965).
(6) J. Behringer and J. Brandmüller, *Ann. Phys. (Leipzig)*, 4, 234 (1959).
(7) L. Rimai, R. G. Kilponen, and D. Gill, *J. Amer. Chem. Soc.*, **92**, 3824 (1970).
(8) D. Gill, R. G. Kilponen, and L. Rimai, *Nature (London)*, in press.
(9) P. Karrer and E. Jucker, "Carotenoids," Elsevier, Amsterdam, 1950.
(10) L. Zechmeister, "Cis-Trans Isomeric Carotenoids, Vitamins A and Arylpolyenes," Academic Press, New York, N. Y., and Springer-Verlag, New York, N. Y., 1962.
(11) W. H. Sebrell, Jr., and R. S. Harris, Ed., "The Vitamins," Vol. 1, Academic Press, New York, N. Y., 1954.
(12) T. Moore, "Vitamin A," Elsevier, Amsterdam, 1957.
(13) I. Heilbron and B. C. L. Weedon, *Bull. Soc. Chim. Fr.*, 83 (1958).
(14) R. Hubbard, *J. Amer. Chem. Soc.*, **78**, 4662 (1956).
(15) L. Jurkowitz, J. N. Loeb, P. K. Brown, and G. Wald, *Nature (London)*, **184**, 614, 617, 620 (1959).
(16) C. D. B. Bridges, *Compr. Biochem.*, **27**, 31 (1967).
(17) E. W. Abrahamson and S. E. Ostroy, *Progr. Biophys.*, 17, 181 (1967).
(18) G. Wald, *Science*, **162**, 230 (1968).
(19) E. R. Blout, M. Fields, and R. Karplus, *J. Amer. Chem. Soc.*, **70**, 194 (1948).
(20) R. G. Sinclair, A. F. McKay, G. S. Myers, and R. N. Jones, *ibid.*, 74, 2578 (1952).
(21) W. D. Celmer and I. A. Solomons, *ibid.*, **75**, 3430 (1953).
(22) K. Lunde and L. Zechmeister, *ibid.*, 77, 1647 (1955).